Published in final edited form as:
Sci Transl Med. 2010 November 10; 2(57): 57ra82. doi:10.1126/scitranslmed.3001510.

TLR9 Differentiates Rapid from Slowly Progressive Forms of Idiopathic Pulmonary Fibrosis

Glenda Trujillo[a], **Alessia Meneghin**[a], **Kevin R. Flaherty**[b], **Lynette M. Sholl**[c], **Jeffrey L. Myers**[a], **Ella A. Kazerooni**[d], **Barry H. Gross**[d], **Sameer R. Oak**[a], **Ana Lucia Coelho**[a], **Holly Evanoff**[a], **Elizabeth Day**[e], **Galen B. Toews**[b], **Amrita D. Joshi**[a], **Matthew A. Schaller**[a], **Beatrice Waters**[e], **Gabor Jarai**[e], **John Westwick**[e], **Steve L. Kunkel**[a], **Fernando J. Martinez**[b], and **Cory M. Hogaboam**[a]

[a]Department of Pathology, University of Michigan Medical School, Ann Arbor, Michigan, USA

[b]Department of Internal Medicine, Division of Pulmonary and Critical Care Medicine, University of Michigan Health System, Ann Arbor, Michigan, USA

[c]Brigham and Women's Hospital, Department of Pathology, Harvard Medical School, Boston, Massachusetts, USA

[d]Department of Radiology, University of Michigan Medical School, Ann Arbor, Michigan, USA

[e]Novartis Institutes of Biomedical Research, Respiratory Disease Area, Horsham, West Sussex, UK

Abstract

Idiopathic pulmonary fibrosis is a generally progressive disorder with highly heterogeneous disease progression. The most common of the idiopathic interstitial pneumonias, idiopathic pulmonary fibrosis is characterized by a steady worsening of lung function and gas exchange cause by diffuse alveolar damage and severe fibrosis. We examined clinical features of patients with idiopathic pulmonary fibrosis to classify them as exhibiting rapid or slowly progressive over the first year of follow-up. We identified differences between the two groups in order to investigate the mechanism of rapid progression. Previous work from our laboratory has demonstrated that Toll-like receptor 9, a pathogen recognition receptor, promotes myofibroblast differentiation in lung fibroblasts cultured from biopsies of patients with idiopathic pulmonary fibrosis. Therefore, we hypothesized that TLR9 functions as both a sensor of pathogenic molecules and a profibrotic signal in rapidly progressive idiopathic pulmonary fibrosis. TLR9 was present at higher concentrations in surgical lung biopsies from rapidly progressive patients than in tissue from normal controls. Fibroblasts from rapid progressors were more responsive to the TLR9 agonist, CpG, than were fibroblasts from control patients. We used a humanized SCID mouse and demonstrated that there was increased fibrosis in murine lungs receiving human lung fibroblasts from rapid progressors than in mice receiving normal fibroblasts. This fibrosis was exacerbated by intranasal CpG challenges. Furthermore, CpG induced the differentiation of blood monocytes into fibrocytes and the epithelial-to-mesenchymal transition of A549 lung epithelial cells. These data suggest that TLR9 may drive the pathogenesis of rapidly progressive idiopathic pulmonary fibrosis and is a potential indicator of this subset of the disease.

Correspondence: Glenda Trujillo, Ph.D., Department of Pathology, State University of New York at Stony Brook, Stony Brook, NY 11794-8691, Phone: 631-444-3940, Fax: 631-444-3424, gtrujillo@notes.sunysb.edu.

Introduction

Idiopathic pulmonary fibrosis (IPF) is a chronic, generally progressive lung disease with high mortality and inadequate and available therapy. It is widely accepted that IPF is initiated by an unknown insult to the lung that leads to irreversible scarring marked by severe alveolar destruction, variable inflammation accompanied by excessive deposition of extracellular matrix, and ultimate loss of normal lung function (1). The pathogenesis of IPF is not completely understood, although persistent fibroblast proliferation and activation are considered to be targetable mechanisms for therapeutic intervention. Fibroblasts are fundamental to tissue homeostasis and normal wound repair through its production of extracellular matrix (ECM) proteins. In fibrosing diseases like IPF, their unregulated proliferation, differentiation into myofibroblasts, and excessive production of ECM leads to destruction of normal interstitial architecture.

There is growing evidence that, in addition to the proliferation of resident fibroblasts, these cells also arise from other cellular sources such as bone-marrow-derived fibrocytes and epithelial cells (2). Fibrocytes can enter damaged tissue through chemokine-dependent mechanism and mature into collagen-producing myofibroblasts(3-6). Moreover, epithelial structures can differentiate into myofibroblasts through epithelial-mesenchymal transition (EMT)(7-10). These proposed mechanisms for the pathogenesis of fibrotic disease are common among all tissues such as the kidney, liver, skin, and lung. Further investigation of the pathways involved may improve the treatment of patients with variable forms of fibrotic diseases.

The disease course of IPF patients is extremely variable, with some patients exhibiting disease stability for prolonged periods of time while other exhibit rapid disease progression (11). Although some IPF patients exhibit gradual physiological decline others experience acute deterioration as a result of acute exacerbation of IPF (AE-IPF)(12). Disease progression in IPF patients has been defined by using a composite approach, which includes physiological progression, AE-IPF and/or all-cause mortality. Rigorous studies aimed at understanding the etiology, risk factors, and pathogenesis of disease progression are required for the accurate treatment, prognosis, and predictors of IPF. A way to predict the disease course during an initial evaluation would have great practical value.

Several hypotheses have been proposed for the etiology of IPF disease progression but no consensus has been reached. An accelerated variant of IPF appears to clinically distinguish rapid progressors from IPF patients who experience a slower or more stable progressive clinical course, however whether rapid progression equates with having a history of an acute exacerbation has not been established (13). In addition, viral infections, especially herpesviruses, have been associated with IPF and may be linked to AE-IPF. Specifically, the prototypic gammaherpesvirus, EBV, has been consistently detected in IPF patients(14-16). The Toll-like receptor system orchestrates the primary recognition of infectious agents which leads to the innate and adaptive immune response. TLR9 recognizes unmethylated CpG DNA motifs present in bacterial and viral DNA, and interacts with gammaherpesvirus to mediate host immunity (17). Furthermore, gammaherpesvirus exacerbates established pulmonary fibrosis in a fluorescein isothiocyanate (FITC) murine model of pulmonary fibrosis (18). Our laboratory has recently reported that enhanced TLR9 expression on pulmonary fibroblasts derived from lung biopsies of patients with IPF drives the in vitro differentiation of myofibroblasts in response to CpG (19). Therefore, we hypothesized that TLR9 may be a predictor of the rapidly progressive form of IPF and may render these patients susceptible to acute exacerbations. We have here tested this hypothesis.

Results

Diagnosis, Sample Collection, and Treatment of IPF Patients IPF patients

We included twenty three patients diagnosed with IPF using a multidisciplinary, clinical/radiological/pathological mechanism (20). Baseline data for each patient in the study included detailed clinical assessment, physiological studies, high resolution computed tomography (HRCT), and surgical lung biopsies (SLBs). Patients were treated with a variety of treatment regimens and followed closely with physiological studies and capture of clinical information during acute events. The physiological criteria used to validate disease progression during the first year of follow-up included a forced vital capacity (FVC) decrease ≥ 10% and a diffusing capacity for carbon monoxide (DLCO) decrease ≥ 15% based on baseline physiological abnormality. Acute exacerbations of IPF were defined using criteria recently proposed by our group (21) or all-cause mortality.

Clinical Features of Rapid and Slowly Progressive Forms of IPF

Ten IPF patients in our cohort exhibited disease progression during the initial one year of follow-up after initial diagnosis while 13 did not; mean time of follow-up for the patients was 1154 ± 603 days. Of the ten patients experiencing progressive disease during the first year of follow-up, eight were characterized as rapid progressors on the basis of physiological parameters (FVC decrease >10%, DLCO decrease >15%), one experienced an acute exacerbation of IPF, and one died of respiratory causes over a time frame longer than usually used to define an acute exacerbation. Overall survival was better in patients who did not compared to those that did exhibit disease progression over the first year of follow-up ($p=0.003$) (Fig. 1A). Table 1 enumerates the clinical, physiological, imaging, and histological features at initial diagnosis baseline. No statistically significant differences were noted in demographics, physiological severity, or HRCT/histological semi-quantitative abnormality as a function of progressive disease. Figure 1B demonstrates representative histology for slow (panels A and B) and rapid progressors (panels C and D). In both groups of patient, the surgical lung biopsies showed heterogeneous interstitial fibrosis with architectural distortion (Fig. 1B A and C) and multifocal fibroblast foci (panels B and D) characteristic of usual interstitial pneumonias (UIP). None of the patients had evidence of acute exacerbation of IPF (diffuse alveolar damage) at the time of surgical lung biopsy.

Because TLR9 is highly expressed in IPF lungs and CpG-ODN can drive a myofibroblast differentiation of IPF lung fibroblasts in vitro (19), we tested whether TLR9 expression differed in rapidly and slowly progressive IPF. We quantitated TLR9 expression in surgical lung biopsies from IPF patients clinically classified as rapid or slow progressors. TLR9 gene expression was elevated in lungs from rapidly progressive IPF patients compared to normal and slow progressors (Fig. 1C). These results were confirmed by immunohistochemical analysis of TLR9 in surgical lung biopsies from rapid and slow progressors, which showed both the intensity and localization of TLR9 protein (Fig. 1D). There was no difference in TLR9 expression based on the criterion used to define individual patient's disease progression. TLR9 protein was increased in the interstitial areas of the lung (Fig. 1D panel c) from rapid progressors as compared to slow progressors. The pronounced TLR9 staining appeared to be localized to the immune cells (Fig. 1D panel a).

CpG-ODN Induces a Fibroblast-like Phenotype in Primary Human Blood Monocytes In Vitro in the Presence of TGFβ

On the basis of our previous findings that CpG induces myofibroblast differentiation of IPF fibroblasts, we investigated whether CpG could also drive a fibroblast-like phenotype in other cell types relevant to the pathogenesis of IPF. Studies from other laboratories have reported that fibroblast-like cells (“fibrocytes”) can arise from purified human CD14+

monocytes under serum-free conditions within 4 days in culture (22-24). This result is in contrast to other reports demonstrating a fibrocyte population devoid of CD14 in human PBMC cultures after 7 days in the presence of serum (24, 25). In these studies, the addition of TGFβ to PBMC cultures promoted fibrocyte differentiation, which is minimally defined by spindle-shaped morphology and collagen 1 expression. Thus, in the present study we tested whether CpG can drive a fibrocyte-like phenotype in purified CD14+ monocytes. Peripheral blood monocytes from healthy human donors were purified for CD14-expressing cells by negative selection that depleted T and B cells, dendritic cells, NK cells, erythrocytes, and stem cells. Purified CD14+ cells were plated in serum-free media in the presence or absence of 10 ng/mL TGFβ for 3 days, after which they were stimulated for an additional day with nothing, control nonstimulatory CpG-ODN (non CpG), CpG-ODN, or a TLR3 agonist (Poly I-C) (Fig. 2A). Morphological assessment by phase- contrast microscopy revealed that monocytes cultured in media alone or in combination with TGFβ maintained a rounded shape typical of a monocytic phenotype (Figure 2B panels a and b). The same phenotype was observed in macrophages stimulated with non CpG (Figure 2B panels c and d) and poly I-C (Figure 2B panels g and h) both in the absence and presence of TGFβ. In contrast, monocytes stimulated with either CpG alone (Figure 2B panel e) or with CpG in the presence of TGFβ (Figure 2B panel f) exhibited a distinct population of elongated, spindle-shaped cells resembling fibrocytes. To determine whether the differences in the cultures corresponded with the induction of fibrocyte markers, RNA was isolated and purified from the adherent cells and subjected to gene expression analysis by quantitative TaqMan real-time PCR. Alpha smooth muscle actin (αSMA) is a specific protein marker expressed primarily on mesenchymal cells such as smooth muscle and fibroblasts, and is typically absent in non-structural cells. Upregulation has been linked to myofibroblast differentiation and, more recently, fibrocyte differentiation. We observed induction of αSMA gene transcript *only* in monocytes stimulated with CpG and not in those treated with other TLR agonists (Fig. 2C panel a). TGFβ did not alter αSMA gene expression in cells that were stimulated with CpG, suggesting that upregulation of αSMA gene expression in our culture system is specific to CpG.

We observed that, in agreement with previous studies from other laboratories, monocytes demonstrate upregulation of collagen 1 when cultured in the presence of TGFβ (Fig. 2C panel b). Unstimulated monocytes also express collagen, which is consistent with previous reports that macrophages indeed express the entire repertoire of collagens (26). Although we did not observe any differences in collagen expression that correlated with the morphological differences we observed (CpG-induced elongated, spindle-shaped cells), these data confirm that TGFβ increases collagen expression in CD14+ monocytes but that this effect may only be limited to TGFβ.

We further tested whether CpG affects collagen protein expression in cultured CD14+ monocytes by immunofluorescence (IF) and flow cytometry. Collagen staining was increased in CD14+ monocytes that were cultured with either TGFβ alone or stimulated with CpG alone in media (Fig. 2D). Treatment with both CpG and TGFβ enhanced collagen 1 staining (panel d), which is consistent with the change in morphology demonstrated in Figure 2B panel f. Furthermore, flow cytometry quantification of collagen-positive CD14+CD45+ monocytes indicates that CpG enhances collagen 1 protein expression in TGFβ-cultured cells (**panel f**).

We next characterized these fibrocyte-like monocytes with flow cytometric analysis. Initial observations of forward and side scatter properties of CD14+ monocytes cultured in the presence or absence of TGFβ confirmed that CpG induces morphological changes that are consistent with a fibroblast-like cell shape. The majority of monocytes cultured in TGFβ alone appeared smaller in size (Fig. 2E). In contrast, monocytes stimulated with CpG in the

presence of TGFβ have a dominant population (72.3% of total cells) comprised of cells with increased forward scatter and side scatter, indicative of increased cellular size and complexity (2E, b).

Monocyte-derived fibrocytes are widely characterized as CD14-negative, and PBMCs lose CD14 expression upon differentiation into fibrocytes (27, 28). Moreover, CD14 is a cell surface co-receptor for lipopolysaccharide (LPS), a bacterial cell wall component, along with TLR4 and MD-2, on macrophages that can be shed during bacterial infections (29, 30). We tested whether the presence or absence of TGFβ affected the CD14+ monocyte population during fibrocyte differentiation in our culture system. After 4 days, >95% of the total cells were CD14- when cultured in media alone, and CpG did not affect the population (Fig. 2E, c). When cultured in media containing TGFβ or TGFβ and CpG, CD14+ monocytes comprise almost 100% of the cell population (2E, d). These results demonstrate that CD14 expression on monocytes is dynamic, and that loss or maintenance of CD14 expression does not necessarily correlate with their fibrocytes differentiation.

We next analyzed CpG effects on the CD14+ and CD14- monocyte population for upregulation of established fibrocytes markers by flow cytometry. We found that in CD14- cells, CpG alone or in combination with TGFβ induced expression of CD45, a hematopoietic marker widely used to characterize fibrocytes (Figure 2E panels e and f). Upregulation of CD45 by CpG was also observed in CD14+ monocytes that were cultured with TGFβ (Figure 2E panel h). No effect on CD45 expression was observed in CD14+ cells cultured in media alone (Figure 2E panel g). Collectively, these data suggest that CpG induces a fibrocyte-like phenotype in CD14+ monocytes as defined by induction of an elongated, spindle-shaped morphology, and upregulation of αSMA, collagen 1 and CD45 protein.

CpG-ODN Induces Epithelial-Mesenchymal Transition in A549 Cells

Based on the CpG-mediated effects observed in monocytes (Figure 2), we postulated that CpG may induce a classic EMT response in epithelial cells. We tested the human adenocarcinoma type II alveolar epithelial cell line, A549, used to investigate TGFβ-driven EMT (31-33), with TGFβ and observed cell spreading and elongation, loss of epithelial cell markers such as E-cadherin, and expression of mesenchymal proteins including αSMA, collagen 1, and Vimentin. Untreated A549 cells after 96 hours in culture media maintained a cobblestone epithelial morphology and growth pattern (Figure 3A panel a). Figure 3A panel b is a representative image of A549 cells cultured with 5 ng/mL for 96 hours and demonstrates TGFβ-induced cell spreading and a fibroblast-like morphology. To test whether CpG can also induce these changes, we treated A549 cells with increasing concentrations of CpG for 24, 48, 72, and 96 hours and assessed morphological changes and expression of EMT markers. CpG treatment induced cell spreading and elongated, spindle-shaped cells in a concentration-dependent manner during a 96-hour treatment (Fig. 3B).

Changes in cell morphology assessed under phase contrast light microscopy were observed as early 24 hours with the lowest concentration of CpG, however the most dramatic effects occurred after 72 and 96 hours. To confirm whether the morphological changes observed with CpG corresponded with EMT, we next isolated RNA from the cultured A549 cells and measured gene expression of EMT markers. CpG stimulated expression of αSMA, with an optimal effect at 200 μg/mL CpG (Fig. 3B, panel a) and expression. CpG treatment of A549 cells also resulted in a concentration-dependent induction of vimentin with an optimal effect at 200 μg/mL CpG (Figure 3B panel b) that is also accompanied by a loss of E-cadherin expression (Figure 3B panel c). In addition, fluorescent immunocytochemistry revealed a dose-dependent induction of collagen 1 by CpG in A549 cells after 96 hours (Figure 3D panels a-e). These data show that CpG induces EMT in lung epithelial cells. To determine whether CpG can also induce an innate immune response from A549 cells (34), we

measured IFNα gene expression after increasing concentrations of CpG. We detected optimal IFNα gene transcript in cells treated with 200 μg/mL (Figure 3D), indicating that the EMT effects observed at this concentration also correlated with an innate immune response.

To determine whether CpG-DNA induction of EMT in A549 cells was TLR9 dependent, we targeted TLR9 protein expression by RNA interference and assessed knockdown before testing CpG-mediated EMT in these cells. A549 cells treated with an siRNA pool consisting of 4 different specific sequences against nothing (non target), the reference protein cyclophillin B, or TLR9 were lysed 96 hours after a 96 hours treatment. TLR9 protein expression was ablated in cells treated with TLR9 siRNA but not non target or cyclophilin B siRNA (Fig. 3E). Moreover, A549 cells at this timepoint appeared similar to those cultured in treatment media plus transfection reagent alone (Figure 3E panel b) and showed no indication of stress response or changes in morphology microscopically in cells cultured with non target siRNA (Figure 3E panel b) or TLR9 siRNA (Figure 3E panel c). After TLR9 protein silencing was confirmed by Western Blot (Figure 3E panel a) in one of the triplicate wells from the same experiment, siRNA-treated A549 cells in the remaining duplicate wells were stimulated with CpG-DNA for additional 72 hours and monitored throughout for changes in morphology. The morphology of A549 cells cultured in treatment media plus transfection reagent appeared unaltered (Figure 3E panel e). Non target siRNA had no effect on inhibiting CpG-mediated EMT, as indicated by cell spreading and elongated, spindle-shaped cells. In contrast, A549 cells treated with TLR9 siRNA failed to demonstrate similar morphological changes (Figure 3E panel g). These cells appeared stressed and apoptotic, which may indicate that complete ablation of TLR9 may drive alternative innate immune responses in alveolar epithelial cells in the presence of CpG-DNA. To further demonstrate that CpG induces EMT in a TLR9-dependent manner, we isolated RNA from the siRNA and CpG-treated cultured A549 cells and measured gene expression of EMT markers. TLR9 silencing by siRNA inhibited CpG-mediated induction of vimentin expression and downregulation of E-cadherin expression, respectively (Fig. 3E).

TLR9 Expression and Response to CpG-ODN is Increased in Rapidly Progressive IPF

Representative lung fibroblasts from surgical lung biopsies obtained from patients exhibiting rapid disease progression were cultured in vitro with media alone or in the presence of a profibrotic stimulus, IL-4, to examine induction of TLR9 gene transcript. Stimulation of fibroblast cell line 204A (rapid progressor) with unmethylated CpG-ODN, a TLR9 agonist, resulted in increased TLR9 expression (Figure 4a) compared to that response observed with cell line 100A (slow progressor) (Figure 4b).

In vitro cytokine production by fibroblasts from rapid and slowly progressing IPF patients was measured in cultured cell supernatants and compared in their responsiveness to CpG-ODN in the presence or absence of IL-4. Since type I interferons are secreted by cells upon effective TLR9 signaling, we measured IFN-α protein in supernatants from cultured fibroblast cell lines (35). Rapidly progressive cell line 204A (Figure 4c) demonstrates enhanced production of IFN-α compared to the slowly progressive line 100A (Figure 4d) when stimulated with CpG in the presence of IL-4. This observation is consistent with the heightened expression of TLR9 by 204A the presence of both CpG-ODN and IL-4 (Figure 4a). Rapidly progressive cell line 204A also demonstrates increased secretion of the profibrotic cytokines PDGF (Figure 4e), MCP-1/CCL2 (Figure 4g), and MCP-3/CCL3 (Figure 2h) when stimulated with both CpG-ODN and IL-4. This is in contrast to the response observed with the slowly progressing line 100A, which does not show a comparable effect on the production of profibrotic cytokines with CpG in the presence of IL-4 (Figure 2f, 2h and 2j). Taken together, these data show a differential expression pattern of TLR9 and response to CpG between lung fibroblasts from rapid and slowly progressive IPF lungs.

Rapidly Progressing Human IPF Fibroblasts Show Increased Fibrogenicity in a Humanized SCID Model of IPF

We used a previously described humanized SCID mouse model to test the fibrogenic potential of human lung fibroblasts from rapid versus slow progressors in vivo (36). Representative lung fibroblasts cultured from rapid or slow progressors were analyzed in vitro (Figure 4) and intravenously transferred into C.B.17SCID/bg mice. On Day 35 after transfer, mice were intranasally challenged with 50 μg CpG-ODN or saline and fibrosis was assessed on Day 63 after transfer (Figure 5A). No pulmonary histopathology was observed in C.B.17SCID/bg mice that received normal pulmonary fibroblasts (Figure 5B panel a). Moreover, no effect was observed in these mice when challenged with CpG on Day 35 (Fig. 5B panel b). Histological assessment of mouse lungs by trichrome stain on day 63 after transfer revealed that rapidly progressive human IPF fibroblasts exhibited collagen deposition and apparently disrupted the the alveolar space as a result of severe interstitial thickening and remodeling (Fig. 5B panel c). Furthermore, fibrosis was markedly enhanced in those lungs that received a CpG challenge on Day 35 (Fig. 5B panel d). This is in contrast to the degree of fibrosis observed in mouse lungs that received slowly progressing human IPF fibroblasts and a CpG challenge. Slowly progressing IPF human lung fibroblasts cause a modest fibrotic response in mouse lungs as assessed on Day 63 after transfer (panel e) that was not enhanced by a CpG stimulus (Fig. 5B panel f). Hydroxyproline, a commonly used marker of de novo collagen synthesis in experimental models of fibrosis, was measured on Day 35 in half lung samples from C.B.17SCID/bg mice that had received IPF human fibroblasts from rapid progressors, and either challenged with saline or CpG on Day 35. CpG challenge significantly increases hydroxyproline content only in mouse lungs transplanted with fibroblasts from rapidly progressive IPF patients (Fig. 5C, a), correlating with the histological assessment of increased collagen deposition in lungs from mice adoptively transferred with rapidly progressive IPF fibroblasts. Moreover, Figure 5C panel b confirms the histology in Figure 5B (panels e and f): CpG challenge does not result in an increase in hydroxyproline content in mouse lungs transplanted with fibroblasts from slowly progressive IPF patients.

Discussion

Idiopathic pulmonary fibrosis (IPF) remains a chronic and fatal lung disease with unmet clinical needs. Increasingly, it has become evident that the disease course in IPF patients is extremely variable with some patients exhibiting relative disease stability for prolonged periods of time while others exhibit rapid disease progression(11). Although some IPF patients exhibit physiological decline others experience acute deterioration, acute exacerbation of IPF (AE-IPF)(12, 21). As such, increasingly disease progression in IPF patients has been defined using a composite approach which includes physiological progression, AE-IPF and/or all cause mortality. Rigorous studies aimed at understanding the etiology, risk factors, and pathogenesis of disease progression is required for the accurate management of IPF. As many current treatment studies emphasize intermediate term outcomes defining disease course during an initial evaluation would have great practical value.

AE-IPF remain poorly understood, and mortality of patients who present with this accelerated phase of the disease face death in period of weeks to a few months. Systematic studies of serum and BAL from patients with AE of IPF are lacking and, as such, no current molecular investigation of the pathogenesis of AE-IPF exists. Though the causes of AE-IPF are unknown, one possible explanation emerges from the detection of EBV in the lungs of IPF patients(14-16): that an innate immune response to viral or bacterial infections may enhance the underlying fibrotic response. Our present study strongly implicates the overexpression of TLR9, a pathogen recognition receptor, for driving rapid progression in

IPF. In this study, our aim was to identify a mechanism of action by which the TLR9 accelerates the fibrotic process through its recognition of CpG DNA.

We report that surgical lung biopsies from rapidly progressive IPF patients clinically exhibit elevated levels of TLR9 gene transcript expression compared to those from stable IPF patients. We provide clinical data from these patients linking TLR9 expression to the rapid or stable phenotype of IPF. Importantly, the definition of clinical progression was defined independently of the presence of TLR9 expression. Those patients experiencing rapid clinical progression were similar to those exhibiting relative stability over the first year of follow-up with regards to demographic characteristics, physiological abnormality, semiquantitative radiological abnormality and pathological abnormality. Not surprisingly, patients exhibiting rapid progression exhibited overall worse survival compared to those with relative stability. Thus, our data suggests that TLR9 is a potential indicator of IPF disease progression. Recently, annexin 1 was identified as a novel autoantigen present in patients with AE-IPF, however it was not addressed whether these patients also possessed a more robust measure of rapidly progressive disease(37). Interestingly, this study reported that inflammatory infiltrates (primarily lymphocytes, neutrophils, and eosinophils) are elevated in the bronchoalveolar lavage of AE-IPF compared to that from stable IPF patients, which had undetectable amounts of these acute inflammatory cells(37). Elevations in neutrophil elastase, the mucin protein KL-6, ST2 protein, IL-8, and alpha defensin have also been previously reported in some patients with AE, suggesting a role for activated T cells and neutrophils(38-42). However, serum levels of these markers did not prove consistent predictors of prognosis(43).

To dissect a mechanism by which TLR9 may function as both a pathogenic sensor and as a profibrotic mediator in IPF, we conducted studies using peripheral blood monocytes from healthy donors. A recent report confirmed that circulating fibrocytes (defined as CD45+Col1+) increase to an average of 15% of peripheral blood leukocytes in IPF patients who were evaluated during episodes of AE-IPF(44). Our current study extends the examination of fibrocytes to identifying them as pathogenic sensors of CpG DNA. Since we did not have access to blood monocytes from IPF patients in the midst of an acute exacerbation, we utilized naïve blood monocytes to investigate the agonistic potential of CpG in the context of fibrosis. Previous studies have demonstrated that bone marrow derived cells (fibrocytes) promote wound repair by migrating to wound sites and serving as a contributing source of myofibroblasts in fibrotic disease. Whether fibrocytes arise from monocytes remains controversial, though TGFβ has been shown to induce the in vitro differentiation of CD14+ monocytes into CD14-/collagen-1 fibrocytes. Our laboratory has previously demonstrated that CpG induces myofibroblast differentiation in cultured lung fibroblasts(19). Moreover, preliminary studies in our laboratory indicated that CD14+ monocytes express significant levels of TLR9 gene transcript, which was in contrast to a previous report by Balmelli et al. that demonstrated expression of TLR7 but not TLR9 in fibrocytes (45). In the current study we tested the hypothesis that CpG may also induce the differentiation of CD14+ monocytes into fibrocytes. Our data demonstrates that CpG treatment results in a hybrid monocyte phenotype, possessing both fibrocyte markers (spindle-shaped morphology, CD45, collagen 1, and α-sma expression) and CD14. We also show that CpG enhances TGFβ-driven differentiation, as demonstrated by increased cell size and increased immunostaining for collagen. These data confirm that monocytes can respond to CpG in a profibrotic manner, and may represent a separate cellular source for contributing to the myofibroblast population in the lung.

Consistent with these results, we also report a CpG-mediated differentiation in the A549 human alveolar epithelial cell line that correlated with a myofibroblastic phenotype. Moreover, our siRNA data suggests that this process is TLR9-dependent, though the exact

mechanism that distinguishes CpG-mediated innate immune responses and EMT in epithelial cells is unknown and under active investigation. It has been previously demonstrated that A549 cells express functionally active TLR9, and that CpG induces an antiapoptotic effect that may promote tumor progression(46). Though we did not measure cytokine secretion in A549 cells in our study, production of MCP-1/CCL2 in response to CpG may also lead to the attraction of immune cells(46). One limitation in our study is that the CpG effects we report are from a transformed cancer cell line, and not in primary alveolar epithelial cells from IPF patients. These studies are currently underway and require further investigation of the mechanism involved. Still, we can speculate that alveolar epithelial cells from IPF lungs are less comparable to normal alveolar epithelial cells as evidenced by increased Wnt/β-catenin signaling shown to drive epithelial cell injury, hyperplasia, and EMT in IPF lungs(47, 48). Indeed, we can conclude from these data that CpG-DNA is recognized by TLR9 expressed on alveolar epithelial cells, promotes EMT, and is a candidate mechanism for the pathogenesis of AE-IPF.

Culturing lung fibroblasts from surgical lung biopsies from IPF patients has been instrumental for establishing a humanized mouse model of IPF(36). In this study, we further extend this model to investigate the role of TLR9 activation in progressive IPF. We determined that lung fibroblasts from patients experiencing a rapidly progressive course demonstrate a hyperresponsiveness to CpG DNA challenge in a SCID model. A single bolus of CpG DNA given intranasally to mice transplanted with rapidly progressive IPF fibroblasts augmented the pulmonary fibrotic response in these mouse lungs, compared to those transplanted with normal or stable IPF fibroblasts. In vitro studies conducted with the same IPF fibroblast cell lines indicated that CpG stimulation results in the enhanced production of profibrotic cytokines from rapidly progressive fibroblasts. Therefore, one hypothesis is that in our SCID model, CpG induces the production of human profibrotic cytokines within the mouse lung and promotes an autocrine response from the human fibroblasts that results in increased fibrosis. These data suggest that CpG recognition by TLR9 within fibroblasts is another potential component of the mechanism by which bacterial or viral constituents augment fibrogenesis during progressive IPF.

TLR9 has recently been implicated in experimental models of other fibrosing diseases. Studies investigating the role of TLR9 in experimental liver fibrosis have demonstrated that TLR9-deficient mice show a protective fibrotic effect in the bile duct ligation (BDL) model of liver fibrosis, indicating a pathophysiological role for bacterial DNA and TLR9 in the development of hepatic fibrosis(49). CpG-ODN was also shown to increase renal fibrosis in a separate study using a murine model for lupus nephritis, as measured by the amount of interstitial fibroblast proliferation in $MRL^{lpr/lpr}$ mice(50). Moreover, other diseases, such as cancers, which result from aberrant cellular activation and proliferation, are susceptible to infectious exacerbations. CpG promotes cellular invasion in breast cancer epithelial cells as well as prostate cells in a TLR9-mediated mechanism(51-53). Chronic hepatitis C virus (HCV) infection that is associated with hepatocellular carcinoma has been recently shown to induce EMT in infected hepatocytes and promote cell invasion and metastasis(54). In our current study we tested whether alveolar epithelial cells respond to bacterial or viral components in a similar manner.

The clinical assessments utilized in our study combined with in vitro and in vivo data acquired from IPF lung fibroblasts strongly implicate TLR9 expression in the alveolar compartment to be an indicator of rapidly progressive IPF. We further demonstrate that expression of TLR9 on immune cells might contribute to the exaggerated wound healing response that might occur in IPF patients exposed to a pathogenic stimulus. We propose that measurement of TLR9 expression in surgical lung biopsies from routine diagnostic tests can be a predictive tool for determining whether IPF patients are susceptible to acute

exacerbations and development of a rapidly progressive phenotype. The presence of bacterial DNA in serum and ascitic fluid is currently under active investigation as an indicator of poor prognosis in patients with liver cirrhosis(55, 56). Though TLR9 was not evaluated in these studies, they provide rationale for measuring unmethylated CpG in serum and BAL from IPF patients, as well as TLR9 expression in IPF patient lung biopsies. Moreover, our current study provides impetus to investigate the therapeutic design of specific TLR9 antagonists. The addition of this diagnostic parameter can potentially identify risk, improve the treatment protocol of IPF patients, and serve as a preventative approach for minimizing susceptibility to acute exacerbations.

Materials and Methods

Mice

All procedures described below were performed in a sterile, laminar environment and were approved by an animal care and use committee at the University of Michigan Medical School. We used adult aged-matched, female C.B-17-scid-beige (C.B-17SCID/bg) mice (Taconic Farms, Germantown, NY). SCID mice were housed in a separate SPF (specific pathogen-free) facility for immunocompromised mice at the University of Michigan Medial School. C.B-17SCID/bg mice have two mutations: the first is the scid mutation, and the second is a beige mutation leading to a major defect in cytotoxic T-cell and macrophage function and a selective impairment in NK cell function.

Human-SCID Model of AE-IPF

Single-cell preparations of IPF/UIP (from clinically-classified rapid or slow progressors) and normal fibroblasts were obtained after trypsinization of 150-cm2 tissue culture flasks and labeled with PKH26 dye according to the manufacturer's directions (Sigma Co., St. Louis, MO). Each labeled fibroblast line was diluted to 2×10^6 cells/ml of phosphate-buffered saline (PBS), and 0.5 ml of this suspension was injected via a tail vain into groups of five to ten SCID mice. Thirty-five days later, all groups of mice were mildly anesthesized and received a single bolus of CpG-ODN (dissolved in sterile saline) or saline by intranasal delivery. Mice were euthanized by cervical dislocation 63 days after the i.v. human pulmonary fibroblast transfer. Whole-lung tissue was dissected at these times for histological and biochemical analysis (see below).

IPF patients

Twenty three patients diagnosed with IPF using a multidisciplinary, clinical/radiological/pathological mechanism(20) were included. Baseline data included detailed clinical assessment, physiological studies, high resolution computed tomography (HRCT), and surgical lung biopsies (SLBs). Semi-quantitative scores of HRCT abnormality were generated using validated methodology(57). Patients were treated with a variety of treatment regimens and followed closely with physiological studies and capture of clinical information during acute events. Using methodology that has been validated disease progression during the first year of follow-up utilized a composite of physiological deterioration(58), the physiological criteria include an FVC decrease ≥ 10% and a DLCO decrease ≥ 15% based on baseline physiological abnormality. Acute exacerbations of IPF were defined using criteria recently proposed by our group(21) or all-cause mortality. This composite approach is now common in NHLBI (ACE IPF) and industry sponsored trials (BUILD 3, Artemis) (www.Clinicaltrials.gov).

Cell Culture and Monocyte Differentiation Assay

Blood was collected from healthy adult volunteers in accordance with University of Michigan Human Research Protection Program (HRPP) (Ann Arbor, MI, USA). PBMCs were isolated from EDTA blood by Ficoll-Paque Plus (GE Healthcare Biosciences, Piscataway, NJ, USA) according to the manufacturer's instructions. CD14+ monocytes were purified by negative selection using the Human Monocyte Isolation Kit II and MACS® LS column separators (Miltenyi Biotec). Briefly, a cocktail of biotin-conjugated antibodies against CD3, CD7, CD16, CD19, CD56, CD123, and CD235a (Glycophorin A), as well as anti-Biotin MicroBeads, yields highly pure unlabeled monocytes obtained by depletion of the magnetically labeled cells. CD14+ monocytes (> 97% pure as detected by FACS) analysis were plated at a density of 2.5×10^6 cells/well in a 6-well plate containing EX-CELL® Hybri-Max™ protein-free medium (Sigma-Aldrich) plus 0.5% sterile BSA with or without 10 ng/mL TGFβ. After 3 days, monocytes were either unstimulated or restimulated with 50 μg/mL sterile CpG-ODN, non-CpG, or poly IC. Twenty-four hours later, monocyte cultures were visualized under phase-contrast microscopy or processed for FACS analysis as described. For gene expression analysis, TriZol reagent was added to each well and RNA extraction was performed according to the manufacturer's instructions. RNA was purified using the RNAeasy RNA cleanup kit (Quiagen) and subjected to on column DNAase digestion (Quiagen). RNA concentration and purity was determined by Nanodrop and confirmed by agarose gel electrophoresis. Purified RNA was subsequently reverse-transcribed into cDNA by rtPCR and similar treatments were pooled for analysis.

A549 Cell Culture and EMT Assay

A549 cells were seeded at a concentration of 40,000 cells/well in 12-well culture plates containing DMEM supplemented with 10% fetal bovine serum, 100 U/ml penicillin and 100 μg/ml streptomycin. Treatments consisted of media alone, CpG (at 5, 10, 50, 100, or 200 μg/mL) or TGFβ (0.1, 0.5, 1, 5, 10ng/mL). Cells were treated for 72 or 96 hrs (as indicated) and then trypsinized for analysis as described.

siRNA Knockdown of TLR9

A549 cells were seeded at a concentration of 10,000 cells/well in 12-well culture plates containing DMEM supplemented with 5% fetal bovine serum. Twenty-four hours later, cells remained untreated or treated with 50 nM ON-TARGET*plus* non-targeting siRNA Pool, 50 nM ON-TARGET*plus* Cyclophilin B Control siRNA Pool, or 50 nM TLR9 ON-TARGET*plus* siRNA SMARTpool (Dharmacon, Thermo Scientific) in DharmaFECT transfection reagent according to the manufacturer's instructions. Cells were incubated for 48 hrs for RNA analysis or 96 hrs for protein analysis to confirm TLR9 knockdown. For CpG-mediated EMT, CpG at the indicated concentration (s) was added to the siRNA-treated cells for 72 or 96 hrs (as indicated) and then trypsinized for analysis as described.

Statistical Analysis

All results are expressed as mean ± SEM or median as appropriate. Baseline characteristics of patients were contrasted by unpaired t-tests or Mann Whitney tests as appropriate. Overall survival characteristics were contrasted between patients experiencing disease progression during the first year of follow-up compared to those that did not using Cox regression analysis. The means between groups at different time points were compared by two-way analysis of variance (59). Individual differences were further analyzed using the unpaired t-test with Tukey-Kramer multiple comparisons test where indicated. Values of $P < 0.1$ (*), $P < 0.01$ (**), and $P < 0.001$ (***) were considered significant.

List of Supplementary Materials

Supplementary Methods

Histological Analysis of Human-SCID Model of IPF—After cervical dislocation, the right lobes from each mouse were dissected, fully inflated with 10% formalin solution, and placed in fresh formalin for 24 hours. Standard histological techniques were used to paraffin-embed each lobe, and 5-μm sections were stained with Masson's trichrome for histological analysis.

Isolation and Culture of Primary Pulmonary Fibroblast Lines—UIP (from clinically-classified rapid or stable progressors) and normal SLBs were finely minced and the dispersed tissue pieces were placed into 150-cm2 cell culture flasks containing DMEM supplemented with 15% fetal bovine serum, 1 mmol/L glutamine, 100 U/ml penicillin and 100 μg/ml streptomycin. All primary lung cell lines were maintained in DMEM-15 at 37°C in a 5% CO2 incubator and were serially passaged a total of five times to yield pure populations of lung fibroblasts as previously described in detail (Hogaboam et al. 2005). All primary fibroblast cell lines from each patient group were used at passages 6 to 10 in the experiments outlined below and all of the experiments were performed under comparable conditions. Each well in a six-well tissue culture plate was seeded with 2.5×10^5 fibroblasts and at the 75% confluence were stimulated for 24 h with media alone or 10 ng/ml of human recombinant IL-4 with or without 100 mM of CpG-ODN (Cell Sciences, CA), a synthetic agonist of TLR9. Twenty-four hours later, cell-free supernatants were collected for analysis.

Preparation of RNA and cDNA from SLBs and Primary Pulmonary Fibroblast Lines—After treatments as describe above, TriZol Reagent (Invitrogen Life Technologies, Carlsbad, CA) was added to each well and total RNA was then prepared according to the manufacturer's instructions. The same process was applied to seven (upper and lower lobes) rapid IPF/UIP, seven (upper and lower lobes) stable IPF/UIP and seven normal SLBs after they were thawed on ice. Purified RNA from SLBs and the fibroblasts was subsequently reverse-transcribed into cDNA using a BRL reverse transcription kit and oligo (dT) 12–18 primers. The amplification buffer contained 50 mmol/L KCl, 10 mmol/L Tris–HCl, pH 8.3, and 2.5 mmol/L $MgCl_2$ (Invitrogen Life Technologies, Carlsbad, CA).

Real-time TaqMan PCR Analysis—Human TLR9, collagen 1, and αsma gene expression was analyzed by a real-time quantitative RT-PCR procedure using an ABI PRISM 7500 Sequence Detection System (PE Applied Biosystems, Foster City, CA). The cDNAs from SLBs samples were analyzed for TLR9 and the cDNAs from cultured monocytes and A549 cells were analyzed for collagen 1 and αsma. GAPDH was used as an internal control. Primers and probe used for TLR9 were purchased from Applied Biosystems. The primers and probes used for collagen 1 were: forward TGGCCTCGGAGGAAACTTT and reverse TCCGGTTGATTTCTCATCATAGC, MGB probe CCCCAGCTGTCTTAT; for αsma: forward GCGTGGCTATTCCTTCGTTACT and reverse GCTACATAACACAGTTTCTCCTTGATG, MGB probe TGAGCGTGAGATTGT. Gene expression was normalized to GAPDH, and the fold increases in targets gene expression was calculated as is indicated for each experiment.

Hydroxyproline Assay—Left lobe samples from each mouse were dissected, homogenized, and biochemically processed as described previously for the hydroxyproline assay (ref). Hydroxyproline concentrations were calculated from a hydroxyproline standard curve (0 to 100 μg of hydroxyproline/ml). The e levels in each sample were normalized to the protein (in mg) present in each sample measured by the Bradford protein assay.

Flow Cytometric Analysis—Monocytes were incubated with Accutase™ (eBiosciences) for 15 minutes after a 4 days treatment to facilitate detachment from cell culture plates and subjected to a previously described protocol for flow cytometric analysis (ref). Monocytes were stained with anti-CD14-PE-Cy7, anti-CD45RO-Pacific Blue, anti-CXCR4-FITC. For TLR9 and collagen staining, monocytes were permeabilized using BD Perm/Wash™ and stained with TLR9-PE and collagen-biotin labeled followed by strepavidin-APC. Cells were analyzed using a FACSCalibur and Cell Quest software (BD Biosciences, San Jose, CA).

Immunofluorescence—Monocytes were added to 8-well glass Labtek (Nunc Inc., Naperville, IL) tissue culture plates at a cell density of 350,000 cells/well containing EX-CELL® Hybri-Max™ protein-free medium (Sigma-Aldrich) containing 0.5% sterile BSA and the indicated treatments for the specified experiment. A549 cells were added to 8-well glass Labtek plates at a density of 20,000 cells/well containing DMEM supplemented with 10% fetal bovine serum, 100 U/ml penicillin and 100 μg/ml streptomycin and the indicated treatments for the specified experiment. Cells were fixed with 4% paraformaldehyde and stained overnight at 4°C with rabbit polyclonal anti-human collagen 1 (Abcam ab292) or rabbit IgG Isotype control (Abcam). After repeated washes in PBS, monocytes were incubated with FITC-conjugated mouse anit-rabbit IgG for 1 h at 4°C. Cells were washed again in PBS, mounted, and visualized using a fluorescent microscope at 40× magnification.

Acknowledgments

This worked was supported, in part, by NIH funding via P50HL56402 (to C.M.H., K.R.F., and F.J.M.) and HL073728 (to C.M.H). The authors also acknowledge the financial support of Novartis Institute of Biomedical Research (NIBR) and Novartis Pharmaceuticals UK limited. G.T. received funding from a NIH Institutional Training Grant (T32) for Pulmonary Research at the University of Michigan Medical School.

References

1. Wynn TA. Cellular and molecular mechanisms of fibrosis. J Pathol. 2008; 214:199. published online EpubJan (10.1002/path.2277 [doi]). [PubMed: 18161745]
2. Laurent GJ, McAnulty RJ, Hill M, Chambers R. Escape from the matrix: multiple mechanisms for fibroblast activation in pulmonary fibrosis. Proc Am Thorac Soc. 2008; 5:311. published online EpubApr 15 (5/3/311 [pii] 10.1513/pats.200710-159DR [doi]). [PubMed: 18403325]
3. Mehrad B, Burdick MD, Zisman DA, Keane MP, Belperio JA, Strieter RM. Circulating peripheral blood fibrocytes in human fibrotic interstitial lung disease. Biochem Biophys Res Commun. 2007; 353:104. published online EpubFeb 2 (S0006-291X(06)02616-7 [pii] 10.1016/j.bbrc.2006.11.149 [doi]). [PubMed: 17174272]
4. Ishida Y, Kimura A, Kondo T, Hayashi T, Ueno M, Takakura N, Matsushima K, Mukaida N. Essential roles of the CC chemokine ligand 3-CC chemokine receptor 5 axis in bleomycin-induced pulmonary fibrosis through regulation of macrophage and fibrocyte infiltration. Am J Pathol. 2007; 170:843. published online EpubMar (170/3/843 [pii] 10.2353/ajpath.2007.051213 [doi]). [PubMed: 17322370]
5. Moore BB, Murray L, Das A, Wilke CA, Herrygers AB, Toews GB. The role of CCL12 in the recruitment of fibrocytes and lung fibrosis. Am J Respir Cell Mol Biol. 2006; 35:175. published online EpubAug (2005-0239OC [pii] 10.1165/rcmb.2005-0239OC [doi]). [PubMed: 16543609]
6. Kisseleva T, Uchinami H, Feirt N, Quintana-Bustamante O, Segovia JC, Schwabe RF, Brenner DA. Bone marrow-derived fibrocytes participate in pathogenesis of liver fibrosis. J Hepatol. 2006; 45:429. published online EpubSep (S0168-8278(06)00247-9 [pii] 10.1016/j.jhep.2006.04.014 [doi]). [PubMed: 16846660]
7. Iwano M, Plieth D, Danoff TM, Xue C, Okada H, Neilson EG. Evidence that fibroblasts derive from epithelium during tissue fibrosis. J Clin Invest. 2002; 110:341. published online EpubAug (10.1172/JCI15518 [doi]). [PubMed: 12163453]

8. Kim KK, Kugler MC, Wolters PJ, Robillard L, Galvez MG, Brumwell AN, Sheppard D, Chapman HA. Alveolar epithelial cell mesenchymal transition develops in vivo during pulmonary fibrosis and is regulated by the extracellular matrix. Proc Natl Acad Sci U S A. 2006; 103:13180. published online EpubAug 29 (0605669103 [pii] 10.1073/pnas.0605669103 [doi]). [PubMed: 16924102]
9. Rygiel KA, Robertson H, Marshall HL, Pekalski M, Zhao L, Booth TA, Jones DE, Burt AD, Kirby JA. Epithelial-mesenchymal transition contributes to portal tract fibrogenesis during human chronic liver disease. Lab Invest. 2008; 88:112. published online EpubFeb (3700704 [pii] 10.1038/labinvest.3700704 [doi]). [PubMed: 18059363]
10. Zeisberg M, Yang C, Martino M, Duncan MB, Rieder F, Tanjore H, Kalluri R. Fibroblasts derive from hepatocytes in liver fibrosis via epithelial to mesenchymal transition. J Biol Chem. 2007; 282:23337. published online EpubAug 10 (M700194200 [pii] 10.1074/jbc.M700194200 [doi]). [PubMed: 17562716]
11. Martinez FJ, Safrin S, Weycker D, Starko KM, Bradford WZ, King TE Jr, Flaherty KR, Schwartz DA, Noble PW, Raghu G, Brown KK. The clinical course of patients with idiopathic pulmonary fibrosis. Ann Intern Med. 2005; 142:963. published online EpubJun 21 (142/12_Part_1/963 [pii]). [PubMed: 15968010]
12. Hyzy R, Huang S, Myers J, Flaherty K, Martinez F. Acute exacerbation of idiopathic pulmonary fibrosis. Chest. 2007; 132:1652. published online EpubNov (132/5/1652 [pii] 10.1378/chest.07-0299 [doi]). [PubMed: 17998366]
13. Selman M, Carrillo G, Estrada A, Mejia M, Becerril C, Cisneros J, Gaxiola M, Perez-Padilla R, Navarro C, Richards T, Dauber J, King TE Jr, Pardo A, Kaminski N. Accelerated variant of idiopathic pulmonary fibrosis: clinical behavior and gene expression pattern. PLoS ONE. 2007; 2:e482. 10.1371/journal.pone.0000482 [doi]. [PubMed: 17534432]
14. Tsukamoto K, Hayakawa H, Sato A, Chida K, Nakamura H, Miura K. Involvement of Epstein-Barr virus latent membrane protein 1 in disease progression in patients with idiopathic pulmonary fibrosis. Thorax. 2000; 55:958. published online EpubNov. [PubMed: 11050267]
15. Stewart JP, Egan JJ, Ross AJ, Kelly BG, Lok SS, Hasleton PS, Woodcock AA. The detection of Epstein-Barr virus DNA in lung tissue from patients with idiopathic pulmonary fibrosis. Am J Respir Crit Care Med. 1999; 159:1336. published online EpubApr. [PubMed: 10194186]
16. Tang YW, Johnson JE, Browning PJ, Cruz-Gervis RA, Davis A, Graham BS, Brigham KL, Oates JA Jr, Loyd JE, Stecenko AA. Herpesvirus DNA is consistently detected in lungs of patients with idiopathic pulmonary fibrosis. J Clin Microbiol. 2003; 41:2633. published online EpubJun. [PubMed: 12791891]
17. Guggemoos S, Hangel D, Hamm S, Heit A, Bauer S, Adler H. TLR9 contributes to antiviral immunity during gammaherpesvirus infection. J Immunol. 2008; 180:438. published online EpubJan 1 (180/1/438 [pii]). [PubMed: 18097045]
18. McMillan TR, Moore BB, Weinberg JB, Vannella KM, Fields WB, Christensen PJ, van Dyk LF, Toews GB. Exacerbation of established pulmonary fibrosis in a murine model by gammaherpesvirus. Am J Respir Crit Care Med. 2008; 177:771. published online EpubApr 1 (200708-1184OC [pii] 10.1164/rccm.200708-1184OC [doi]). [PubMed: 18187693]
19. Meneghin A, Choi ES, Evanoff HL, Kunkel SL, Martinez FJ, Flaherty KR, Toews GB, Hogaboam CM. TLR9 is expressed in idiopathic interstitial pneumonia and its activation promotes in vitro myofibroblast differentiation. Histochem Cell Biol. 2008; 130:979. published online EpubNov (10.1007/s00418-008-0466-z [doi]). [PubMed: 18633634]
20. Flaherty KR, King TE Jr, Raghu G, Lynch JP 3rd, Colby TV, Travis WD, Gross BH, Kazerooni EA, Toews GB, Long Q, Murray S, Lama VN, Gay SE, Martinez FJ. Idiopathic interstitial pneumonia: what is the effect of a multidisciplinary approach to diagnosis? Am J Respir Crit Care Med. 2004; 170:904. published online EpubOct 15 (10.1164/rccm.200402-147OC [doi] 200402-147OC [pii]). [PubMed: 15256390]
21. Collard HR, Moore BB, Flaherty KR, Brown KK, Kaner RJ, King TE Jr, Lasky JA, Loyd JE, Noth I, Olman MA, Raghu G, Roman J, Ryu JH, Zisman DA, Hunninghake GW, Colby TV, Egan JJ, Hansell DM, Johkoh T, Kaminski N, Kim DS, Kondoh Y, Lynch DA, Muller-Quernheim J, Myers JL, Nicholson AG, Selman M, Toews GB, Wells AU, Martinez FJ. Acute exacerbations of idiopathic pulmonary fibrosis. Am J Respir Crit Care Med. 2007; 176:636. published online EpubOct 1 (200703-463PP [pii] 10.1164/rccm.200703-463PP [doi]). [PubMed: 17585107]

22. Pilling D, Buckley CD, Salmon M, Gomer RH. Inhibition of fibrocyte differentiation by serum amyloid P. J Immunol. 2003; 171:5537. published online EpubNov 15. [PubMed: 14607961]

23. Shao DD, Suresh R, Vakil V, Gomer RH, Pilling D. Pivotal Advance: Th-1 cytokines inhibit, and Th-2 cytokines promote fibrocyte differentiation. J Leukoc Biol. 2008; 83:1323. published online EpubJun (jlb.1107782 [pii] 10.1189/jlb.1107782 [doi]). [PubMed: 18332234]

24. Hong KM, Belperio JA, Keane MP, Burdick MD, Strieter RM. Differentiation of human circulating fibrocytes as mediated by transforming growth factor-beta and peroxisome proliferator-activated receptor gamma. J Biol Chem. 2007; 282:22910. published online EpubAug 3 (M703597200 [pii] 10.1074/jbc.M703597200 [doi]). [PubMed: 17556364]

25. Yang L, Scott PG, Giuffre J, Shankowsky HA, Ghahary A, Tredget EE. Peripheral blood fibrocytes from burn patients: identification and quantification of fibrocytes in adherent cells cultured from peripheral blood mononuclear cells. Lab Invest. 2002; 82:1183. published online EpubSep. [PubMed: 12218079]

26. Schnoor M, Cullen P, Lorkowski J, Stolle K, Robenek H, Troyer D, Rauterberg J, Lorkowski S. Production of type VI collagen by human macrophages: a new dimension in macrophage functional heterogeneity. J Immunol. 2008; 180:5707. published online EpubApr 15 (180/8/5707 [pii]). [PubMed: 18390756]

27. Abe R, Donnelly SC, Peng T, Bucala R, Metz CN. Peripheral blood fibrocytes: differentiation pathway and migration to wound sites. J Immunol. 2001; 166:7556. published online EpubJun 15. [PubMed: 11390511]

28. Gomperts BN, Strieter RM. Fibrocytes in lung disease. J Leukoc Biol. 2007; 82:449. published online EpubSep (jlb.0906587 [pii] 10.1189/jlb.0906587 [doi]). [PubMed: 17550974]

29. Moreno C, Merino J, Ramirez N, Echeverria A, Pastor F, Sanchez-Ibarrola A. Lipopolysaccharide needs soluble CD14 to interact with TLR4 in human monocytes depleted of membrane CD14. Microbes Infect. 2004; 6:990. published online EpubSep (10.1016/j.micinf.2004.05.010 [doi] S1286-4579(04)00188-1 [pii]). [PubMed: 15345230]

30. Sandanger O, Ryan L, Bohnhorst J, Iversen AC, Husebye H, Halaas O, Landro L, Aukrust P, Froland SS, Elson G, Visintin A, Oktedalen O, Damas JK, Sundan A, Golenbock D, Espevik T. IL-10 enhances MD-2 and CD14 expression in monocytes and the proteins are increased and correlated in HIV-infected patients. J Immunol. 2009; 182:588. published online EpubJan 1 (182/1/588 [pii]). [PubMed: 19109192]

31. Rho JK, Choi YJ, Lee JK, Ryoo BY, Na II, Yang SH, Kim CH, Lee JC. Epithelial to mesenchymal transition derived from repeated exposure to gefitinib determines the sensitivity to EGFR inhibitors in A549, a non-small cell lung cancer cell line. Lung Cancer. 2009; 63:219. published online EpubFeb (S0169-5002(08)00298-5 [pii] 10.1016/j.lungcan.2008.05.017 [doi]). [PubMed: 18599154]

32. Illman SA, Lehti K, Keski-Oja J, Lohi J. Epilysin (MMP-28) induces TGF-beta mediated epithelial to mesenchymal transition in lung carcinoma cells. J Cell Sci. 2006; 119:3856. published online EpubSep 15 (jcs.03157 [pii] 10.1242/jcs.03157 [doi]). [PubMed: 16940349]

33. Kasai H, Allen JT, Mason RM, Kamimura T, Zhang Z. TGF-beta1 induces human alveolar epithelial to mesenchymal cell transition (EMT). Respir Res. 2005; 6:56. 1465-9921-6-56 [pii] 10.1186/1465-9921-6-56 [doi]. [PubMed: 15946381]

34. Ronni T, Matikainen S, Sareneva T, Melen K, Pirhonen J, Keskinen P, Julkunen I. Regulation of IFN-alpha/beta, MxA, 2′,5′-oligoadenylate synthetase, and HLA gene expression in influenza A-infected human lung epithelial cells. J Immunol. 1997; 158:2363. published online EpubMar 1. [PubMed: 9036986]

35. Osawa Y, Iho S, Takauji R, Takatsuka H, Yamamoto S, Takahashi T, Horiguchi S, Urasaki Y, Matsuki T, Fujieda S. Collaborative action of NF-kappaB and p38 MAPK is involved in CpG DNA-induced IFN-alpha and chemokine production in human plasmacytoid dendritic cells. J Immunol. 2006; 177:4841. published online EpubOct 1 (177/7/4841 [pii]). [PubMed: 16982926]

36. Pierce EM, Carpenter K, Jakubzick C, Kunkel SL, Flaherty KR, Martinez FJ, Hogaboam CM. Therapeutic targeting of CC ligand 21 or CC chemokine receptor 7 abrogates pulmonary fibrosis induced by the adoptive transfer of human pulmonary fibroblasts to immunodeficient mice. Am J Pathol. 2007; 170:1152. published online EpubApr (170/4/1152 [pii] 10.2353/ajpath.2007.060649 [doi]). [PubMed: 17392156]

37. Kurosu K, Takiguchi Y, Okada O, Yumoto N, Sakao S, Tada Y, Kasahara Y, Tanabe N, Tatsumi K, Weiden M, Rom WN, Kuriyama T. Identification of annexin 1 as a novel autoantigen in acute exacerbation of idiopathic pulmonary fibrosis. J Immunol. 2008; 181:756. published online EpubJul 1 (181/1/756 [pii]). [PubMed: 18566442]
38. Mukae H, Iiboshi H, Nakazato M, Hiratsuka T, Tokojima M, Abe K, Ashitani J, Kadota J, Matsukura S, Kohno S. Raised plasma concentrations of alpha-defensins in patients with idiopathic pulmonary fibrosis. Thorax. 2002; 57:623. published online EpubJul. [PubMed: 12096207]
39. Tajima S, Oshikawa K, Tominaga S, Sugiyama Y. The increase in serum soluble ST2 protein upon acute exacerbation of idiopathic pulmonary fibrosis. Chest. 2003; 124:1206. published online EpubOct. [PubMed: 14555548]
40. Ziegenhagen MW, Zabel P, Zissel G, Schlaak M, Muller-Quernheim J. Serum level of interleukin 8 is elevated in idiopathic pulmonary fibrosis and indicates disease activity. Am J Respir Crit Care Med. 1998; 157:762. published online EpubMar. [PubMed: 9517588]
41. Akira M, Sakatani M, Hara H. Thin-section CT findings in rheumatoid arthritis-associated lung disease: CT patterns and their courses. J Comput Assist Tomogr. 1999; 23:941. published online EpubNov-Dec. [PubMed: 10589572]
42. Yokoyama A, Kohno N, Hamada H, Sakatani M, Ueda E, Kondo K, Hirasawa Y, Hiwada K. Circulating KL-6 predicts the outcome of rapidly progressive idiopathic pulmonary fibrosis. Am J Respir Crit Care Med. 1998; 158:1680. published online EpubNov. [PubMed: 9817725]
43. Shinoda H, Tasaka S, Fujishima S, Yamasawa W, Miyamoto K, Nakano Y, Kamata H, Hasegawa N, Ishizaka A. Elevated CC Chemokine Level in Bronchoalveolar Lavage Fluid Is Predictive of a Poor Outcome of Idiopathic Pulmonary Fibrosis. Respiration. 2009 published online EpubMar 6 (000207617 [pii] 10.1159/000207617 [doi]).
44. Moeller A, Gilpin SE, Ask K, Cox G, Cook D, Gauldie J, Margetts PJ, Farkas L, Dobranowski J, Boylan C, O'Byrne PM, Strieter RM, Kolb M. Circulating Fibrocytes Are an Indicator for Poor Prognosis in Idiopathic Pulmonary Fibrosis. Am J Respir Crit Care Med. 2009 published online EpubJan 16 (200810-1534OC [pii] 10.1164/rccm.200810-1534OC [doi]).
45. Balmelli C, Alves MP, Steiner E, Zingg D, Peduto N, Ruggli N, Gerber H, McCullough K, Summerfield A. Responsiveness of fibrocytes to toll-like receptor danger signals. Immunobiology. 2007; 212:693. S0171-2985(07)00114-3 [pii] 10.1016/j.imbio.2007.09.009 [doi]. [PubMed: 18086371]
46. Droemann D, Albrecht D, Gerdes J, Ulmer AJ, Branscheid D, Vollmer E, Dalhoff K, Zabel P, Goldmann T. Human lung cancer cells express functionally active Toll-like receptor 9. Respir Res. 2005; 6:1. 1465-9921-6-1 [pii] 10.1186/1465-9921-6-1 [doi]. [PubMed: 15631627]
47. Konigshoff M, Balsara N, Pfaff EM, Kramer M, Chrobak I, Seeger W, Eickelberg O. Functional Wnt signaling is increased in idiopathic pulmonary fibrosis. PLoS ONE. 2008; 3:e2142. 10.1371/journal.pone.0002142 [doi]. [PubMed: 18478089]
48. Kim KK, Wei Y, Szekeres C, Kugler MC, Wolters PJ, Hill ML, Frank JA, Brumwell AN, Wheeler SE, Kreidberg JA, Chapman HA. Epithelial cell alpha3beta1 integrin links beta-catenin and Smad signaling to promote myofibroblast formation and pulmonary fibrosis. J Clin Invest. 2009; 119:213. published online EpubJan (36940 [pii] 10.1172/JCI36940 [doi]). [PubMed: 19104148]
49. Gabele E, Muhlbauer M, Dorn C, Weiss TS, Froh M, Schnabl B, Wiest R, Scholmerich J, Obermeier F, Hellerbrand C. Role of TLR9 in hepatic stellate cells and experimental liver fibrosis. Biochem Biophys Res Commun. 2008; 376:271. published online EpubNov 14 (S0006-291X(08)01629-X [pii] 10.1016/j.bbrc.2008.08.096 [doi]). [PubMed: 18760996]
50. Anders HJ, Vielhauer V, Eis V, Linde Y, Kretzler M, Perez de Lema G, Strutz F, Bauer S, Rutz M, Wagner H, Grone HJ, Schlondorff D. Activation of toll-like receptor-9 induces progression of renal disease in MRL-Fas(lpr) mice. FASEB J. 2004; 18:534. published online EpubMar (10.1096/fj.03-0646fje [doi] 03-0646fje [pii]). [PubMed: 14734643]
51. Ilvesaro JM, Merrell MA, Li L, Wakchoure S, Graves D, Brooks S, Rahko E, Jukkola-Vuorinen A, Vuopala KS, Harris KW, Selander KS. Toll-like receptor 9 mediates CpG oligonucleotide-induced cellular invasion. Mol Cancer Res. 2008; 6:1534. published online EpubOct (6/10/1534 [pii] 10.1158/1541-7786.MCR-07-2005 [doi]). [PubMed: 18922969]

52. Ilvesaro JM, Merrell MA, Swain TM, Davidson J, Zayzafoon M, Harris KW, Selander KS. Toll like receptor-9 agonists stimulate prostate cancer invasion in vitro. Prostate. 2007; 67:774. published online EpubMay 15 (10.1002/pros.20562 [doi]). [PubMed: 17373717]

53. Merrell MA, Ilvesaro JM, Lehtonen N, Sorsa T, Gehrs B, Rosenthal E, Chen D, Shackley B, Harris KW, Selander KS. Toll-like receptor 9 agonists promote cellular invasion by increasing matrix metalloproteinase activity. Mol Cancer Res. 2006; 4:437. published online EpubJul (4/7/437 [pii] 10.1158/1541-7786.MCR-06-0007 [doi]). [PubMed: 16849519]

54. Battaglia S, Benzoubir N, Nobilet S, Charneau P, Samuel D, Zignego AL, Atfi A, Brechot C, Bourgeade MF. Liver cancer-derived hepatitis C virus core proteins shift TGF-Beta responses from tumor suppression to epithelial-mesenchymal transition. PLoS ONE. 2009; 4:e4355. 10.1371/journal.pone.0004355 [doi]. [PubMed: 19190755]

55. Zapater P, Frances R, Gonzalez-Navajas JM, de la Hoz MA, Moreu R, Pascual S, Monfort D, Montoliu S, Vila C, Escudero A, Torras X, Cirera I, Llanos L, Guarner-Argente C, Palazon JM, Carnicer F, Bellot P, Guarner C, Planas R, Sola R, Serra MA, Munoz C, Perez-Mateo M, Such J. Serum and ascitic fluid bacterial DNA: a new independent prognostic factor in noninfected patients with cirrhosis. Hepatology. 2008; 48:1924. published online EpubDec (10.1002/hep.22564 [doi]). [PubMed: 19003911]

56. El-Naggar MM, Khalil el SA, El-Daker MA, Salama MF. Bacterial DNA and its consequences in patients with cirrhosis and culture-negative, non-neutrocytic ascites. J Med Microbiol. 2008; 57:1533. published online EpubDec (57/12/1533 [pii] 10.1099/jmm.0.2008/001867-0 [doi]). [PubMed: 19018026]

57. Kazerooni EA, Martinez FJ, Flint A, Jamadar DA, Gross BH, Spizarny DL, Cascade PN, Whyte RI, Lynch JP 3rd, Toews G. Thin-section CT obtained at 10-mm increments versus limited three-level thin-section CT for idiopathic pulmonary fibrosis: correlation with pathologic scoring. AJR Am J Roentgenol. 1997; 169:977. published online EpubOct. [PubMed: 9308447]

58. Flaherty KR, Andrei AC, Murray S, Fraley C, Colby TV, Travis WD, Lama V, Kazerooni EA, Gross BH, Toews GB, Martinez FJ. Idiopathic pulmonary fibrosis: prognostic value of changes in physiology and six-minute-walk test. Am J Respir Crit Care Med. 2006; 174:803. published online EpubOct 1 (200604-488OC [pii] 10.1164/rccm.200604-488OC [doi]). [PubMed: 16825656]

59. Ivanova L, Butt MJ, Matsell DG. Mesenchymal transition in kidney collecting duct epithelial cells. Am J Physiol Renal Physiol. 2008; 294:F1238. published online EpubMay (00326.2007 [pii] 10.1152/ajprenal.00326.2007 [doi]). [PubMed: 18322023]

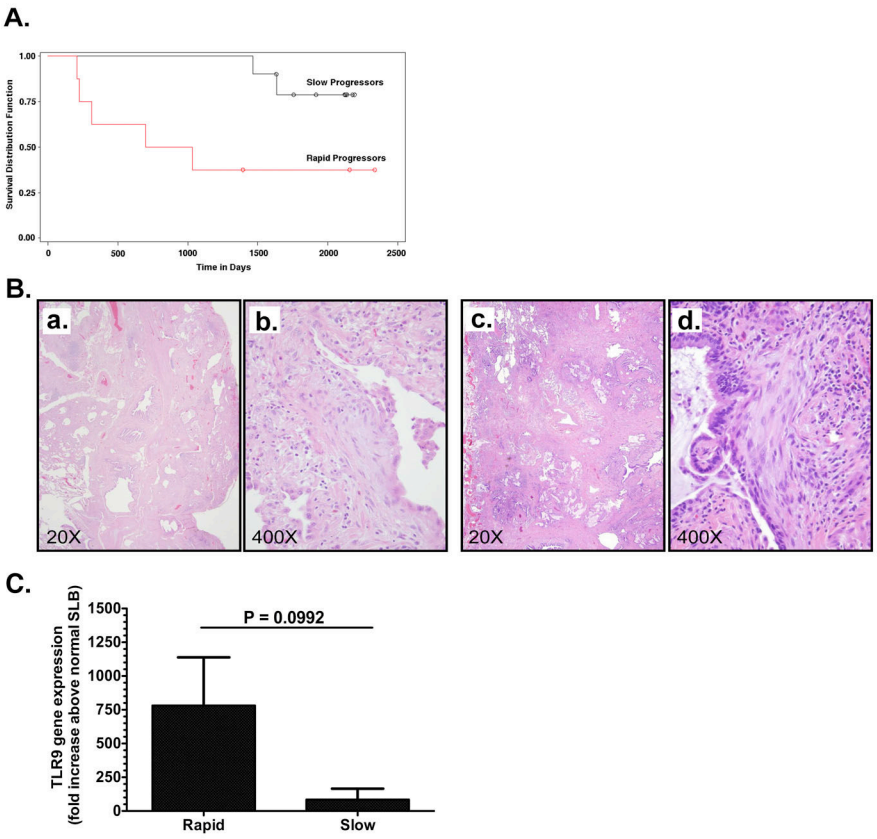

Figure 1. Clinical Features of Patients with Rapid and Slowly Progressive Forms of IPF and TLR9 Expression

A. The survival of IPF patients classified as rapid (red line) or slow progressors (black line). **B.** Representative histology of IPF in a patient with slow (**a,b**) and rapid (**c,d**) progression shown at 20× and 400× magnification. **C.** Quantitative TaqMan PCR analysis of TLR9 gene expression in upper lobe SLBs from rapid and slow progressors. The data shown are the mean of all the combined upper lobe mRNA values compared to the mean of normal SLBs mRNA values (standardized to GAPDH housekeeping gene). The error bar shows the SEM of all the data in the rapid (n=10) and stable (n=13) progressor patient groups. The two-tailed P value was determined by the unpaired t test with Welch correction. **D.** Representative immunohistochemical staining of TLR9 in SLBs from a total of 7 slow (**a**) and 5 rapid (**c**) progressors shown at 20× magnification. Corresponding fields stained with isotype control (IgG) shown in **b** and **d**.

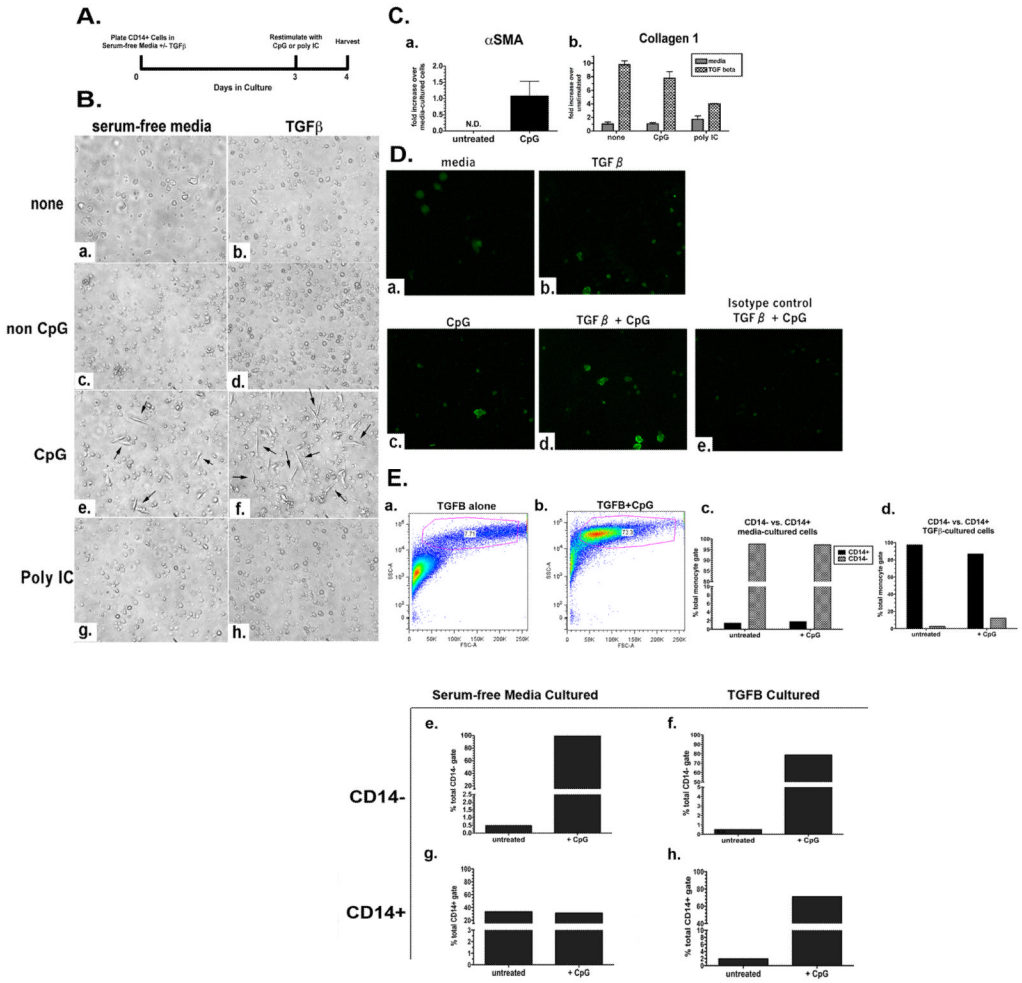

Figure 2. Induction by CpG of CD14+ Human Monocytes to Differentiate into Fibrocyte-like Cells. A

Experimental scheme for the in vitro differentiation of CD14+ monocytes. **B.** Photomicrographs of monocytes cultured in serum-free media or serum-free media containing 10 ng/ml TGFβ and stimulated with nothing **(a,b)**, 50 μg/mL non CpG **(c,d)**, 50 μg/mL CpG **(e,f)**, or 50 μg/mL poly IC **(g, h)** on Day 3. **C.** qRT-PCR analysis of fibrocyte markers. αSMA gene expression in monocytes cultured for 3 d in serum-free media +/- CpG for 24 h **(a)**. Collagen 1 gene expression in monocytes cultured for 3 d in serum-free media or TGFβ, +/- CpG or poly I:C **(b)**. **D.** Fluorescent ICC for collagen 1 in monocytes (40× magnification) cultured in serum-free media **(a)** or TGFβ **(b)**; serum-free media + CpG **(c)**, or TGFβ + CpG **(d)**. Isotype control for monocytes cultured in TGFβ + CpG **(e)**. Representative (n=3) FC for collagen 1 protein as percent of CD14+ cells in CD45+ gate from monocytes cultured in serum-free media or TGFβ, and serum-free media + CpG or TGFβ + CpG **(f)**. **E.** Forward and side scatter FC of monocytes cultured in serum-free media containing TGFβ **(a)** or TGFβ + CpG **(b)**. Representative (n=3) FC for CD14 as percent of total cells from monocytes cultured in serum-free media **(c)** or monocytes cultured in serum-free media containing TGFβ **(d)** stained with anti-CD14. **F.** Representative (n=3) FC for CD45 as percent of CD14- cells from monocytes cultured in serum-free media **(e)** or monocytes cultured in serum-free media containing TGFβ **(f)** stained with anti-CD45 and gated with respect to CD14 expression. Representative data (n=3) is graphed as percent of CD14+ cells from monocytes cultured in serum-free media **(g)** and monocytes cultured in

serum-free media containing TGFβ **(h)** stained with anti-CD45 and gated with respect to CD14 expression.

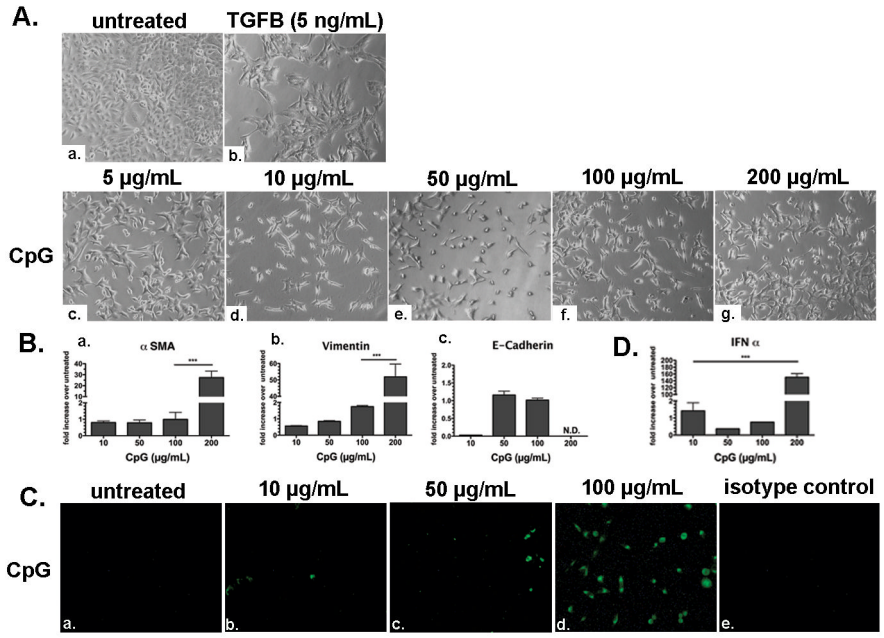

Figure 3. CpG-induced EMT in Human A549 Cells

A. Representative photomicrographs (n=5) of A549 cells cultured in media (DMEM + 10% FCS) **(a)**, TGFβ **(b)**, and increasing CpG concentrations of 5 μg/mL **(c)**, 10 μg/mL **(d)**, 50 μg/mL **(e)**, 100 μg/mL **(f)**, and 200 μg/mL **(g)** for 96 h. **B.** qRT-PCR analysis of αSMA **(a)**, vimentin **(b)**, and e-cadherin **(c)** in A549 cells cultured with increasing concentrations of CpG for 96 hours. **C.** qRT-PCR analysis of IFNα in A549 cells cultured with increasing concentrations of CpG for 96 h. **D.** Fluorescent ICC for collagen 1 in A549 cells (40× magnification) that were cultured for 96 h in media **(a)**, 10 μg/mL CpG **(b)**, 50 μg/mL CpG **(c)**, and 100 μg/mL CpG **(d)**. Isotype control for collagen 1 antibody using cells cultured with 100 μg/mL CpG **(e)**. **E.** siRNA knockdown of TLR9 in A549 cells in a CpG EMT assay: Western Blot analysis of TLR9 protein and β-actin loading control in A549 cell lysates after siRNA treatment with a non targeting control siRNAs, cyclophilin B control siRNAs **(a)**, and TLR9 siRNAs; photomicrographs of A549 cells before CpG-DNA treatment cultured in media and transfection agent alone **(b)**, with non target siRNA **(c)**, and with TLR9 siRNA **(d)**; representative photomicrographs (n=4) of A549 cells after siRNA treatment and stimulated with media and transfection agent alone **(e)**, non target siRNA + 75 μg/ml CpG **(f)**, and TLR9 siRNA + 75 μg/ml CpG-DNA for 72 hrs **(g)**; qRT-PCR analysis of vimentin **(h)** and e-cadherin **(i)** in siRNA-treated A549 cells and cultured with 75 μg/ml CpG for 72 hours. Data are mean ± SD. *** $p < 0.0001$.

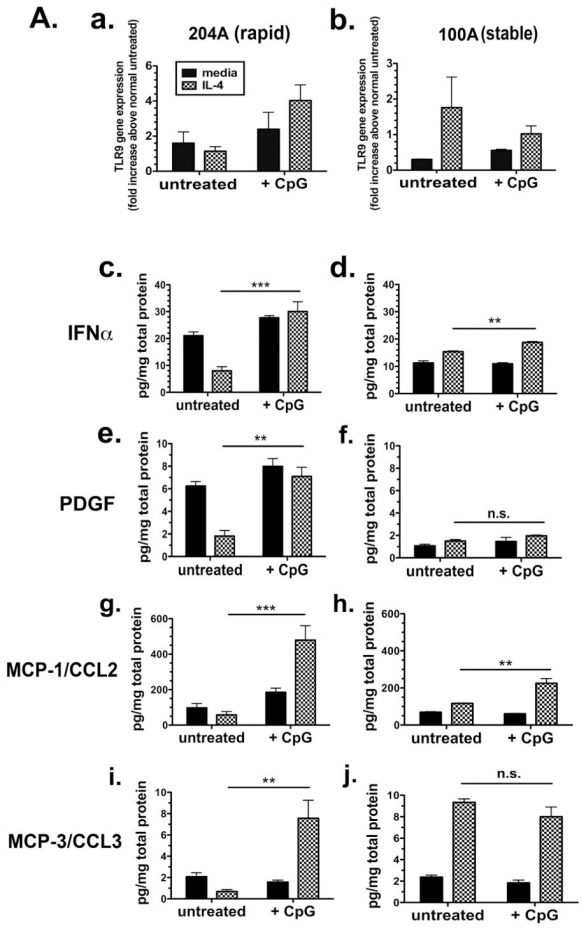

Figure 4. TLR9 Expression in Rapid and Slowly Progressive IPF Lung Fibroblasts and Response to CpG

A. qRT-PCR analysis of TLR9 gene expression in representative rapid UIP/IPF (n=5-8) **(a)** and slow IPF (n=5-8) **(b)** fibroblast cell lines treated for 24 h without (untreated) or with CpG-ODN (10 μg/ml) in the presence or absence of IL-4 (10 ng/ml). Fold increase is calculated within each group of disease compared with the respective untreated fibroblasts. Bioplex analyses of rapid or slow IPF fibroblast conditioned media for IFNα (**c and d**), PDGF (**e and f**), MCP-1/CCL2 (**g and h**), and MCP-3/CCL3 (**i and j**). Fibroblast cell lines were treated for 24 h without (untreated) or with CpG-ODN (10 μg/ml) in presence or absence of IL-4 (10 ng/ml). Data is representative of at least 5 slow IPF and 5 rapid IPF fibroblast cell lines. Data are mean ± SEM. ** $p<0.001$ and *** $p < 0.0001$.

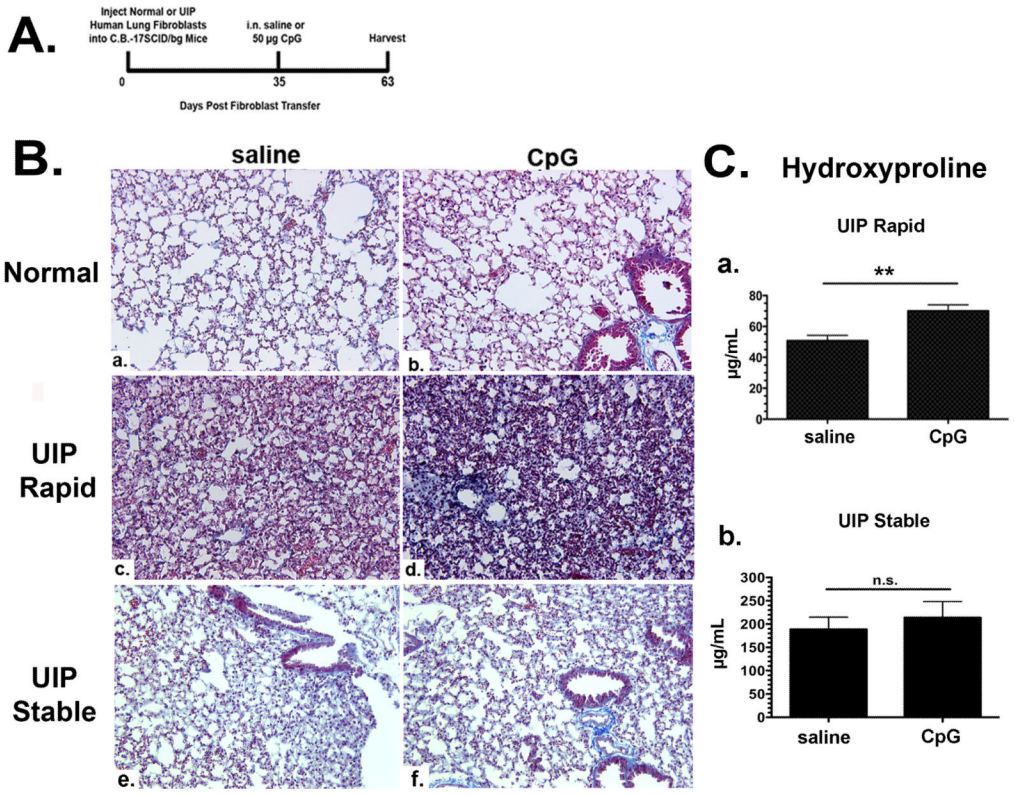

Figure 5. Exacerbation of Fibrosis by CpG in a Human-SCID Mouse Model of IPF Induced by Rapidly Progressive Human Lung Fibroblasts

A. Experimental scheme for establishing a human-SCID model of AE-IPF. **B.** Representative mouse lung sections stained with Masson's trichrome to depict degree of fibrosis from mice that received normal human lung fibroblasts and intranasally challenged on Day 35 with saline **(a)** or CpG **(b)**, rapid UIP/IPF human lung fibroblasts intranasally challenged on Day 35 with saline **(c)** or CpG **(d)**, and slow UIP/IPF human lung fibroblasts intranasally challenged on Day 35 with saline **(e)** or CpG **(f)**. **C.** Hydroxyproline levels in half lung homogenates from saline-challenged or CpG-challenged mice that received rapid UIP/IPF human lung fibroblasts **(a)** and stable UIP/IPF human lung fibroblasts **(b)**. Data are mean ± SEM from five mice at each time point. Data are mean ± SEM. ** $p<0.001$.

Table 1
Clinical Features of Patients with Rapid Versus Slowly Progressive IPF

Feature	Rapid Progressor (n=8)	Slow Progressor (n=10)	P Value
Demographic			
Age	64 ± 7	64 ± 6	0.9
Gender (m/f)	6/2	8/2	0.8
Physiological			
FVC (% pred)	63.4 ± 13.9	73.2 ± 17.5	0.18
DLCO (% pred)	42.3 ± 17.8	58.9 ± 19.0	0.09
HRCT			
Alveolar	1.52 ± 0.8	1.70 ± 0.7	0.67
Interstitial	1.16 ± 0.6	0.89 ± 0.3	0.3
Histological			
HC score (median)	2	1.5	0.61
Max. HC score (median)	2	2	0.7